(17) Huff, J. E., "Plant/Operations Progress", No. 4, 1982.

A COMPUTER MODEL FOR SIZING TWO-PHASE EMERGENCY RELIEF SYSTEMS, VALIDATED AGAINST DIERS* LARGE SCALE TEST DATA

H. H. Klein**

A one-dimensional computer model of two-phase chemically-reacting flow with vapor disengagement has been validated against DIERS large scale venting tests. The model has been applied to evaluation of emergency pressure relief systems for runaway chemical reactors and for vessels exposed to fire. The program has also been used to size rupture discs to prevent runup to detonation in a reactor and pipeline containing detonation gases.

DIERS   Chemical Reactions
Two-Phase   Foamy Liquid Disengagement
Computer Model   Nonfoamy Liquid Disengagement

INTRODUCTION

JAYCOR was contracted by the Design Institute for Emergency Relief Systems (DIERS) organization to analyze the majority of the data from the DIERS venting tests. The objective of the study was to develop insights into the nature of the two-phase venting process and to understand the mechanisms controlling the venting in order to design safe, but not overly conservative relief vents, for chemical reactors. The tests selected by DIERS for analysis spanned a variety of initial and physical conditions ranging in pressure, vessel size, vent type, vent location, and test fluid.

This paper summarizes the work done by JAYCOR on the analysis of the selected DIERS Phase large scale tests.

JAYCOR has performed the analysis by applying its one-dimensional computer model of liquid-vapor flow to simulate the venting from the vessel and vent systems. The program accounts for the liquid and vapor mass lost from the system during the venting, the rate of boiling (and condensation), the mass flux throughout the vessel and vent, and the change in energy of the liquid and

vapor due to runaway chemical reactions and/or system depressurization. The program solves partial differential equations in space and time for mass, momentum and energy of the liquid-vapor mixture as well as an equation for the relative motion between the liquid and vapor (vapor disengagement).

The one-dimensional model assumes that there is no variation of any of the parameters across the diameter of the the vessel and vent. The model does calculate the variation along the axis of the vessel and vent of all of the relevant parameters, i.e., pressure, temperature, chemical composition, void fraction, and velocities. It also determines how the spatial variations change in time as the venting proceeds.

The JAYCOR method of calculating all of the features of the flow simultaneously in the entire vessel and vent system during a runaway event determines the two-phase choking conditions at flow constrictions and vent line ends automatically, without resort to ad hoc choking models.

Another important consideration in the design of relief vents is the rate at which the vapor and liquid phases flow past or disengagement from each other. If the vapor can slip by or disengage from the liquid at an appreciable rate, the size of the relief vent will be smaller than if the vapor and liquid flow together (homogeneous flow). By accounting for the disengagement between the phases, less conservative (and less costly) relief systems can be designed. The JAYCOR model does account for the disengagement between the vapor and liquid in both the vessel and vent and is unique in this regard. The rate of disengagement used in the model has been calibrated against the DIERS large scale test data.

In the JAYCOR model the disengagement is determined as a function of the local voidage, and the disengagement varies as the mixture vents. Since the flow in the vessel and vent is calculated simultaneously in the model, the disengagement is taken to vary continuously from vessel bottom to vent line end, and no distinction is made between separate disengagement regimes in the vessel and vent.

DESCRIPTION OF THE MODEL

In two-phase flow, the assumption of a single pseudo-fluid limits the range of applicability of the model to homogeneous situations. Only in highly agitated states can the phases remain in such intimate contact that mechanical and thermodynamic equilibrium be maintained. Under less violent conditions gravitational or inertial differences between the phases lead to a net relative velocity that can markedly change the flow quantities, especially the void fraction, from that predicted by a homogeneous treatment. Similarly, many engineering applications involve the presence of liquid and vapor at considerably different temperatures, such as in coolant injection, and it is the details of the heat transfer process that is of interest. Again, an equilibrium treatment is inadequate.

JAYCOR has developed a transient, nonequilibrium model of two-phase flow that includes a quantitative description of the flow regime. The model allows for a smooth transition between flow regimes, and the corresponding interphase mass, momentum, and energy are calculated without reference to a flow map. The model of the interphase momentum transfer has been calibrated against the DIERS large scale test data.

Mixture Formulation

The starting point of the analysis is the formally averaged conservation equations of mass, momentum and energy Ref. [1]. Since the vapor and liquid phases during relief remain near equilibrium (equal phase velocities, equal phase temperatures, and pressures at local saturation), we have formulated the model in terms of mixture variables and variables that describe the deviations from equilibrium Ref. [2,3].

Mixture Equations

MASS

$$\frac{\partial \rho_m}{\partial t} + \frac{\partial}{\partial x}(\rho_m u_m) = 0 \tag{1}$$

MOMENTUM

$$\frac{\partial}{\partial t}(\rho_m u_m) + \frac{\partial}{\partial x}\left(\rho_m u_m^2 + \rho_m x_g x_\ell u_r^2\right) = -\frac{\partial P_m}{\partial x} + F_{wm} - \rho_m g + \frac{\partial}{\partial x}\tau_m \tag{2}$$

ENERGY

$$\frac{\partial}{\partial t}(\rho_m h_m) + \frac{\partial}{\partial x}\left[\rho_m h_m u_m + \rho_m(x_\ell h_g - x_g h_\ell)u_r\right] = \frac{\partial}{\partial x} q_m + Q_{wm}$$

$$+ \frac{\partial P_m}{\partial t} + u_m \frac{\partial P_m}{\partial x} + W_r \tag{3}$$

The equations describing the deviation from equilibrium are:

Deviation Equations

VELOCITY

$$(\rho_g x_\ell + \beta \rho_\ell)\frac{\partial u_r}{\partial t} + u_m \frac{\partial u_r}{\partial x} = -C_{22}u_r + S_2 + D_2 \tag{4}$$

TEMPERATURE

$$\frac{\theta_g \theta_\ell}{\rho_m C_{Pm}}\left[\frac{\partial}{\partial t}(\rho_m T_r) + \frac{\partial}{\partial x}(\rho_m u_m T_r)\right] = C_{31}(\rho_m x_r) - C_{33}(\rho_m T_r)$$

$$+ S_3 + D_3 \tag{5}$$

For situations where the vapor and liquid are in equilibrium, such as runaway chemical reactions and pressure relief, Equation (5) can be replaced by:

VAPOR LIQUID EQUILIBRIUM

$$P_i = \gamma_i x_i P_i^o(T_m) \tag{6}$$

$$P_m = \sum_i P_i \tag{7}$$

Additional equations required to close the system of equations are:

EQUATIONS OF STATE

$$\rho_{gi} = \frac{P_m W_i}{R\, T_g\, m} \tag{8}$$

$$\rho_{\ell i} = \rho_{\ell i}(T_m) \tag{9}$$

$$\frac{1}{\rho_m} = \sum_i \frac{x_{gi}}{\rho_{gi}} + \sum_i \frac{x_{\ell i}}{\rho_{\ell i}} \tag{10}$$

$$h_m = \sum_i x_{gi} h_{gi}(T_m) + x_{\ell i} h_{\ell i}(T_m) = h_g + h_\ell \tag{11}$$

SPECIES MASS CONSERVATION

$$\frac{\partial \rho_m x_i}{\partial t} + \frac{\partial}{\partial x}\left[\rho_m x_i u_m + \rho_m(x_{gi} x_\ell - x_{\ell i} x_g)u_r\right] = R_{ij} \tag{12}$$

where

$$x_i = x_{gi} + x_{\ell i}$$

$$x_g = \sum_i x_{gi}$$

$$x_\ell = \sum_i x_{\ell i}$$

An important element in the JAYCOR model is the relation determining the relative motion or disengagement between the liquid and vapor. In the DIERS study, we have found that the amount of vapor motion relative to the liquid controls the behavior of the venting, and the details of the venting are sensitive to this relative motion. In a bubbly liquid the friction by the liquid on the bubble surface determines the rate of the bubble rises in the liquid. The friction decreases markedly as the bubbles merge into larger bubbles. The void fraction increases, and the rate of flow of the vapor past the liquid increases. As the void fraction increases further, the liquid can break into droplets and the vapor becomes the continuous phase. The drag between the droplets and the vapor becomes large and the disengagement decreases. A number of functional forms of the frictional drag between vapor and liquid were tested in the JAYCOR model. Two were chosen, one appropriate to foamy liquids and one appropriate to nonfoamy liquids, as giving the best results over the range of DIERS large scale tests.

CALCULATION RESULTS

The JAYCOR model analyzed the majority of the DIERS large scale venting tests. In this Section we present the results of calculations of a representative number of the tests and compare the computer results with the data. The description of the tests discussed in this section are shown in the following table.

Test	Fluid	Volume (ℓ)	Vent Type	Vent Location	L/D	Vent Diam. (mm)	Initial Pressure (kPa)	Initial Void Fraction	Fluid Type
T-1C	H_2O	2190	Nozzle	Top	1	50.8	505	0.05	Nonfoamy
T-12A	H_2O (det)	2190	Nozzle	Top	1	50.8	510	0.05	Foamy
T-23A	Ethyl-benzene	32	Long Vent	Top	425	26.7	540	0.16	Nonfoamy
V200 RC-2	Rubber Cement/ Hexane	200	Long Vent	Bottom	30	52.6	546	109 kg	Foamy
ICRE 2000-5	Styrene/ Poly-styrene/ Ethyl-benzene	2190	Long Vent	Top	340	76.2	561	0.08	Nonfoamy

Test T-1C

Test T-1C was a water blowdown test through a nozzle at the top of the vessel. Figure 1a shows the vessel pressure versus time, and Figure 1b shows the vessel averaged void fraction versus time for this test.

The solid lines in Figures 1a and 1b show the calculated venting behavior using the nonfoamy liquid disengagement model. There is good agreement with the data (circles) over the time span of the venting. The calculated venting behavior assuming the foamy liquid disengagement model is indicated by the dashed lines. The venting behavior assuming no disengagement between phases (homogeneous flow) gave an even larger mass loss rate and smaller pressure decay rate than the two curves shown. For this test the calculations indicate that the water vents as a nonfoamy liquid.

Figure 1c shows spatial profiles of the void fraction at various times during the calculation of the nonfoamy fluid relief. The vapor disengagement and the static head has caused a variation in void fraction from the vessel bottom to top. The curve at 176 sec shows a significant variation of 0.05 to 0.5 from bottom to top. The average void fraction is quite different from the void fraction at the vent entrance, which is near unity at all times.

Test T-12A

Test T-12A test was identical to test T-1C except that a foaming agent was added to the water before the vessel was pressurized. Figure 2a shows the vessel pressure versus time, and Figure 2b shows the vessel averaged void fraction versus time for this test.

The solid lines in Figures 2a and 2b show the calculated venting using the foamy liquid disengagement model. There is good agreement with the data (circles). The dashed lines show the calculated venting using the nonfoamy
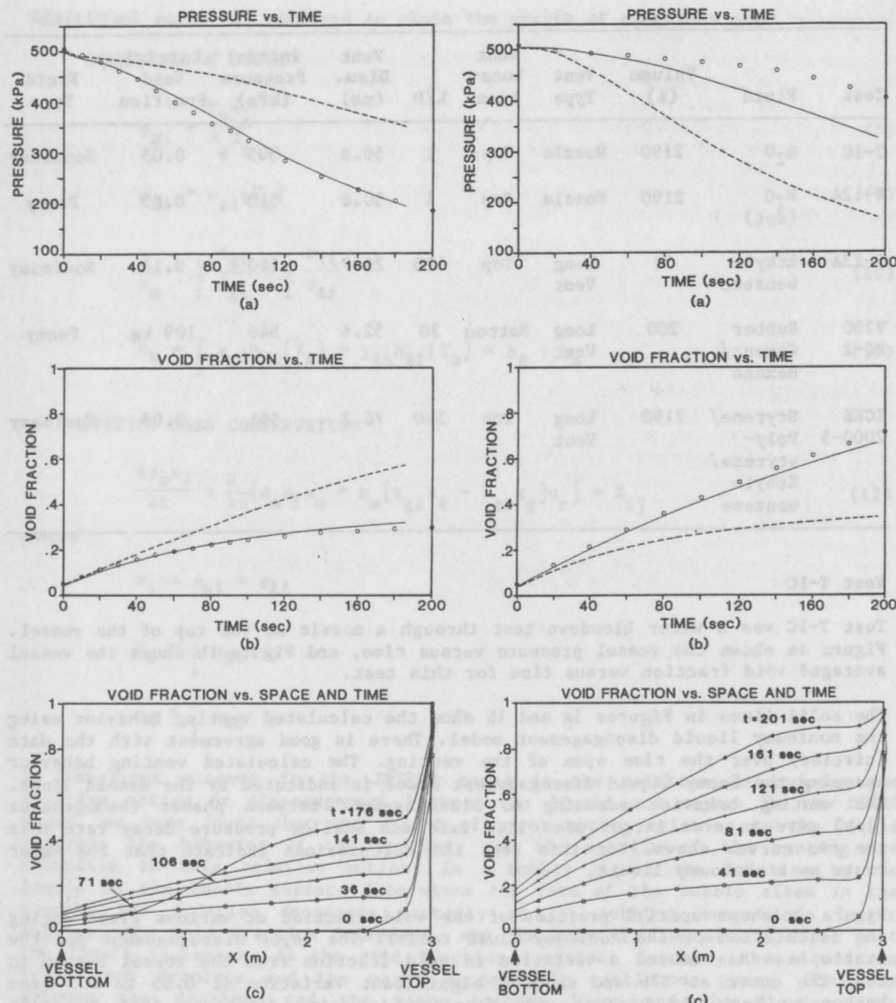
PRESSURE vs. TIME

VOID FRACTION vs. TIME

VOID FRACTION vs. SPACE AND TIME

Figure 1. Test T-1C.

PRESSURE vs. TIME

VOID FRACTION vs. TIME

VOID FRACTION vs. SPACE AND TIME

Figure 2. Test T-12A.

liquid disengagement model. The calculated venting for a homogeneous fluid would give a larger mass loss rate and lower pressure decay rate than given even by the nonfoamy fluid venting. The calculations indicate that the water with detergent added vents as a foamy fluid.

Figure 2c shows spatial profiles of the void fraction at various times during the calculation of the foamy fluid relief. The curves show significant variation in void fraction from vessel bottom to top (not homogeneous) even though the disengagement is small. The average void fraction is quite different from the void fraction of near unity at the vent.

Test T-23A

Test T-23A was a blowdown test with ethylbenzene through a long vent at the top of the vessel. Figure 3a shows the vessel pressure versus time, and Figure 3b shows the vessel averaged void fraction versus time for this test.

The solid lines in Figures 3a and 3b show the calculated venting behavior using the nonfoamy liquid disengagement model. A two-phase, turbulent wall drag model was also used in the calculation to model the flow in the long vent line. The figures indicate that there is good agreement with the data (circles) over the span of the venting.

Figures 3c shows spatial profiles of the void fraction at various times during the calculation. The curves show significant variation in void fraction from vessel bottom to top. The void fraction entering the vent is close to unity, which is considerably different from the average values.

Test V200 RC-2

Test V200 RC-2 was a blowdown involving a high viscosity rubber cement-hexane mixture. The venting was from the bottom of the vessel through a long vent line. Figure 4a shows the vessel pressure versus time, and Figure 4b shows the vessel averaged void fraction versus time for this test.

Figures 4a and 4b show the calculated venting behavior using the foamy liquid disengagement model. A wall drag model based on the viscosity of rubber cement was used in this calculation to model the flow in the long vent. The figures indicate good agreement with the pressure and the void fraction data (circles) over the span of the blowdown.

Figure 4c shows spatial profiles of the void fraction at various times during the calculation. The curves show significant variation in void fraction from vessel bottom to top. The mixture entering the vent is predominantly liquid, and the liquid flashes as it enters and flows along the vent.

Test ICRE 2000-5

Test ICRE 2000-5 was a chemically reacting test involving the polymerization of styrene. At actuation the mixture was 50% styrene, 35% polystyrene, and 15% ethylbenzene. The relief was through a long vent at the top of the vessel.

Figure 5a shows the results of the calculation of vessel pressure using the foamy liquid disengagement model. The calculated pressure rises to 1200 kPa, whereas the data (circles) show a rise to almost 700 kPa. Figure 5b shows the calculated vessel average void fraction with this model. The calculation gives too large a liquid loss and too large a void fraction compared to the data.

Figures 6a and 6b show the calculated results assuming the vapor and liquid behaves as a homogeneous fluid. At 80 sec the reaction has runaway with the calculated pressure rising above 1400 kPa. Assuming that the fluid is homogeneous to size the vent for this case would give a much larger vent than is necessary.

Figures 7a and 7b show the calculated results using the nonfoamy fluid disengagement model. The calculated pressure and void fraction are in closer agreement with the data with this assumption.
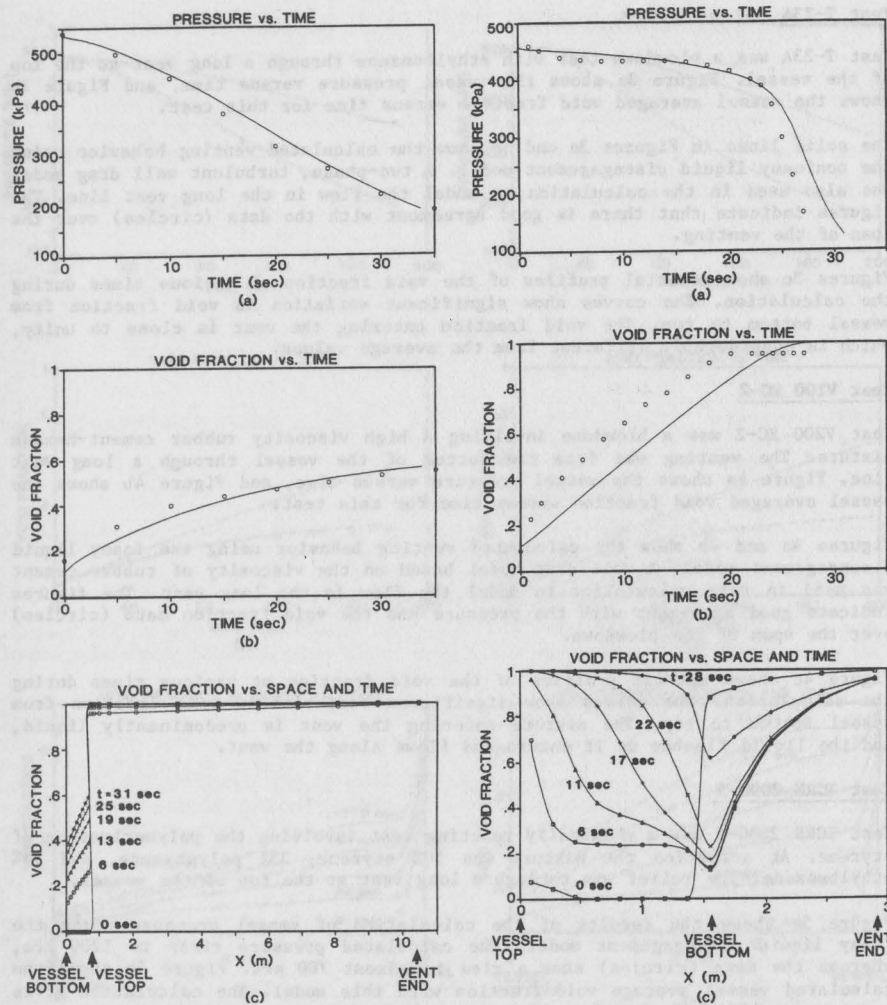
Figure 3. Test T-23A.   Figure 4. Test V200 RC-2.

The plot in Figure 7c shows spatial profiles of the void fraction at various times during the calculation using the nonfoamy disengagement model. The curves show a large variation in void fraction from vessel bottom to top. The void fraction at the vent is essentially unity, which is significantly different from the average values.
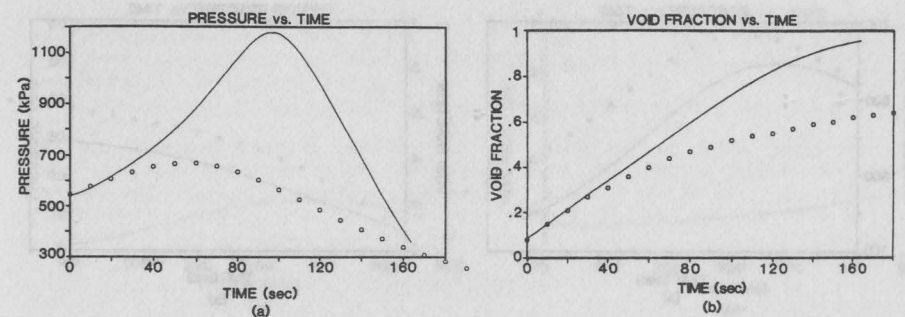
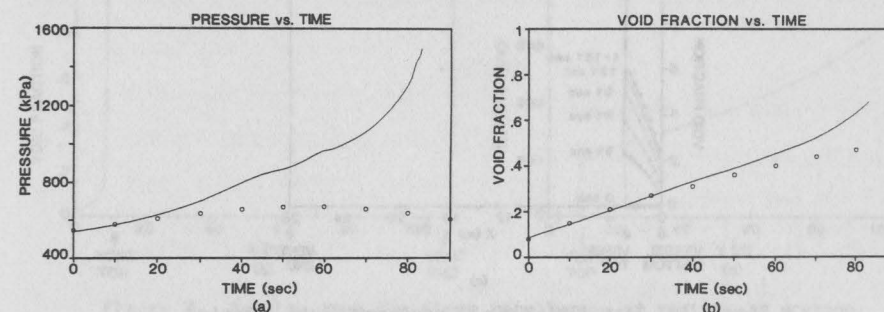Figure 5. Test ICRE 2000-5, foamy fluid behavior.

Figure 6. Test ICRE 2000-5, homogeneous fluid behavior.

FIRE EXPOSURE TO A SOLVENT STORAGE VESSEL:
VENT SIZING WITH THE NONFOAMY DISENGAGEMENT MODEL

As an example of the use of the computer model, we calculate the overpressure in a solvent storage vessel exposed to fire.

The pertinent parameters for the calculation were the following:

Vessel Diameter	6.5 ft
Vessel Height	10.0 ft
Vessel Volume	2483 gal
Vessel Surface Area	242 ft^2
Vessel Height/Diameter	1.54
Vent Diameter	4 in.
Vent Length	100 ft
Heat of Vaporization	242 Btu/lb
Heat Flux	20,000 Btu/hr-ft^2

The remaining properties of the liquid and vapor were those of acetone. The disengagement model of slip between the liquid and the vapor was taken to be appropriate for nonfoamy liquids. In the calculations the heating was applied to the surface of both the vessel and the vent, and the pressure at the end of the vent was assumed to be one atmosphere. A two-phase turbulent wall drag model was used to model the flow in the vent.

PRESSURE vs. TIME

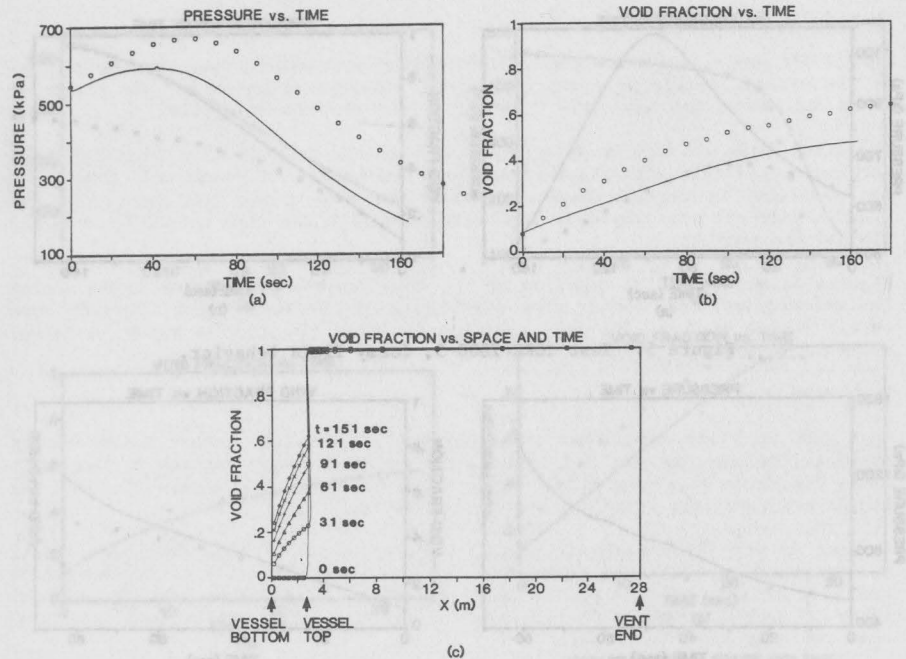VOID FRACTION vs. TIME

VOID FRACTION vs. SPACE AND TIME

Figure 7. Test ICRE 2000-5, nonfoamy fluid behavior.

The heat flux times the vessel surface area divided by the heat of vaporization yields a projected boiling rate of 20,000 lb/hr.

In the calculation the initial pressure was 2.5 psig, and the initial temperature was 140°F, which is the saturation temperature. Figure 8a is a plot of the vessel pressure versus time from this calculation and shows the pressure reaches a maximum of approximately 15 psig at 375 sec and decays gradually thereafter.

Figure 8b is a plot of the vessel void fraction versus time and shows that the void fraction increased from 0.12 to 0.27 during the calculation. That is, 15% of the liquid was lost. The density of the liquid was approximately 6.6 lb/gal, so that 2350 lb or 357 gal of liquid were lost. Since both the vessel and vent were heated, almost all of the liquid entering the vent was boiled.

The loss of 2350 lb of liquid in 560 sec implies an average boiling rate of 15,000 lb/hr. This boiling rate is much less than the projected rate of 20,000 lb/hr which was estimated from the heat flux, surface area, and heat of vaporization. This difference between the actual rate and the projected boiling rate can be attributed to the fact that a small amount of heat went to raising the temperature of the liquid from 140°F to 162°F. Thus, all of the input heat does not go toward the boiling of the liquid.

Although the average flow rate is less than 20,000 lb/hr, the maximum instantaneous rate was 19,300 lb/hr at 375 sec.
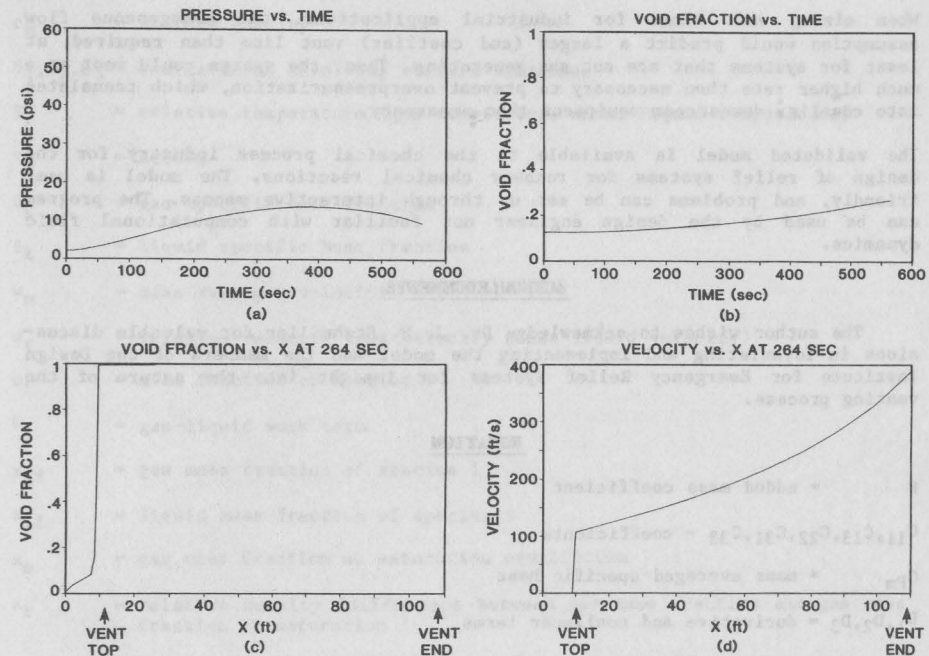
PRESSURE vs. TIME

VOID FRACTION vs. TIME

VOID FRACTION vs. X AT 264 SEC

VELOCITY vs. X AT 264 SEC

Figure 8. Results from the first calculation of venting of acetone through a 100 ft, 4 in. vent line. The heat flux is 20,000 Btu/hr-ft^2.

Figure 8c is a spatial plot of the void fraction from vessel bottom to the vent end at 264 sec. The plot confirms that the void fraction jumps to almost unity in the vent line, i.e., the venting is almost all vapor. Although the plot does not indicate it, a small amount of liquid survives to the end of the vent.

Figure 8d is a spatial plot of the velocity in the vessel and vent at 264 sec and shows the velocity increasing along the vent line. This increase is due to the boiling and expansion of the vapor in the line.

This calculation is consistent with the API recommendation of assuming all vapor venting for determining relief vent sizes for vessels containing volatile liquids which are exposed to fire.

CONCLUSIONS

A mathematical model of venting of runaway chemical reactions has been presented. We have applied the model to the analysis of the DIERS large scale venting tests and have found that the use of one vapor-liquid disengagement function characteristic of nonfoamy liquids and one function characteristic of foamy liquids accurately reproduce the data over a wide range of vessels, fluids, and vent types. For the tests studied the model predicted some level of vapor disengagement, even for foamy systems. This implies that relief vent size predictions using a homogeneous flow model in the vessel and vent would be overly conservative.

When sizing vent lines for industrial applications, the homogeneous flow assumption would predict a larger (and costlier) vent line than required, at least for systems that are not gas generating. Thus, the system could vent at a much higher rate than necessary to prevent overpressurization, which translates into costlier downstream equipment than necessary.

The validated model is available to the chemical process industry for the design of relief systems for runaway chemical reactions. The model is user friendly, and problems can be set up through interactive menues. The program can be used by the design engineer not familiar with computational fluid dynamics.

ACKNOWLEDGEMENTS

The author wishes to acknowledge Dr. J. H. Stuhmiller for valuable discussions in formulating and implementing the model and the members of the Design Institute for Emergency Relief Systems for insight into the nature of the venting process.

NOTATION

β = added mass coefficient

$C_{11}, C_{13}, C_{22}, C_{31}, C_{33}$ = coefficients

C_{Pm} = mass averaged specific heat

D_1, D_2, D_3 = derivative and nonlinear terms

F_{wm} = wall drag force per unit volume

g = gravity acceleration

γ_i = activity coefficient of species i

h_{gi} = enthalpy of gas species i

$h_{\ell i}$ = enthalpy of liquid species i

h_m = mass averaged enthalpy

P_i = partial pressure of species i

P_m = pressure acting on the mixture

P_i^o = pure component vapor pressure of species i

q_m = heat flux

Q_{wm} = heat per unit volume from the walls

R_{ij} = production of species i from reaction with species j

R_g = universal gas constant

ρ_{gi} = gas density of species i

$\rho_{\ell i}$ = liquid density of species i

ρ_m = mixture density

S_1, S_2, S_3 = source terms involving mixture variables

T_r = relative temperature (gas temperature minus liquid temperature)

τ_m = stress

θ_g = gas specific heat fraction

θ_ℓ = liquid specific heat fraction

u_m = mass averaged velocity

u_r = relative velocity (gas velocity minus liquid velocity)

w_i = mole fraction of species i

W_r = gas-liquid work term

x_{gi} = gas mass fraction of species i

$x_{\ell i}$ = liquid mass fraction of species i

x_m = gas mass fraction at saturation equilibrium

x_r = relative quality (difference between gas mass fraction and gas mass fraction at saturation)

X_i = mole fraction of species i in the liquid phase.

REFERENCES

1. J. A. Boure and J. M. Delhaye, "General Equations and Two-Phase Flow Modeling," Handbook of Multiphase Systems, pp. 1-36 – 1-95, Gad Hetstroni, Editor, McGraw Hill, New York, 1982.

2. J. H. Stuhmiller, "A Review of the Rational Approach to Two-Phase Flow Modeling," Electric Power Research Institute, Palo Alto, NP-197, July 1976.

3. J. H. Stuhmiller, "A Dynamic Flow Regime Model of Two-Phase Flow," Electric Power Research Institute (Topical Report-in-Progress).